Eur Biophys J (2002) 31: 365–372
DOI 10.1007/s00249-002-0220-8

ARTICLE

Anurag Varshney · S. Kavitha · M.K. Mathew

Modulation of voltage sensitivity by N-terminal cytoplasmic residues in human Kv1.2 channels

Received: 17 January 2002 / Revised: 22 February 2002 / Accepted: 1 March 2002 / Published online: 25 May 2002

Abstract Potassium channels are now among the best understood membrane proteins and most salient functions have been mapped onto distinct portions of the protein. The detailed mechanism by which movement of the voltage sensor is transduced into channel opening is yet to be understood. We have constructed chimæras from our collection of human voltage-gated potassium channels and expressed them in *Xenopus* oocytes. Here we report on a chimæric construct, 1N/2, generated by swapping the N-terminal cytoplasmic residues of hKv1.1 onto the transmembrane body of hKv1.2. This chimæra functions as a classic outward rectifier but with a 25 mV hyperpolarizing shift in the mid-point of channel activation. The conductance of oocytes expressing this construct decreases significantly on depolarizing beyond +5 mV, unlike full-length hKv1.2. Other parameters such as ionic selectivity and charybdotoxin blockage are unaffected in making the chimæra. These observations suggest that the introduction of the "foreign" chain from hKv1.1 does not cause a large-scale perturbation of channel structure. Loss of the N-terminus from hKv1.2 is not responsible for the shift in voltage dependence, as a truncation construct, Δ75N2, starting at the splice junction, has the same voltage-dependence as full-length hKv1.2. Both constructs show a maximum in their conductance-voltage curves. This decline in conductance on extensive depolarization may arise due to perturbations to the machinery that locks channels into their open state on depolarization. Taken together with our observations on other N-terminal swapped chimæras, our data imply that N-terminal residues can interact with transmembrane regions and perturb the machinery mediating voltage-dependent channel gating.

Keywords Voltage sensitivity · Potassium channel · *Xenopus* oocyte · Chimæra

Presented at the Australian Biophysical Society Meeting, 2001

A. Varshney · S. Kavitha · M.K. Mathew (✉)
Laboratory of Membrane Biophysics,
National Centre for Biological Sciences, TIFR,
UAS-GKVK Campus, Bangalore 560 065, India
E-mail: mathew@ncbs.res.in
Tel.: +91-80-3636421 ext. 3270
Fax: +91-80-3636662/675

Introduction

The waveforms of action potentials in excitable cells are sculpted by the characteristics of the repolarizing potassium currents. Voltage-gated potassium channels are tetrameric proteins, each subunit of which has six transmembrane helices and a re-entrant loop that lines the aqueous pore. Their relatively small size, wide range of functions and sensitivity of electrophysiological analysis make them excellent models for the correlation of structure with function in membrane proteins. Mutagenesis experiments and domain swaps have led to the assignment of specific functional roles to various regions (Yellen 1998). The key elements identified are the inactivation gate, the voltage sensor and the pore loop. Rapidly inactivating channels have a ball-like structure at the N-terminus of their cytoplasmic domains which physically blocks open channels, causing inactivation by the "ball and chain" mechanism (Antz et al. 1997; Zagotta et al. 1990). The fourth transmembrane segment (S4) is positively charged and has been shown to move in response to changes in transmembrane electrical potential (Bezanilla 2000; Cha et al. 1999; Mannuzzu et al. 1996), thus serving as a voltage sensor. Analysis of the "gating charge" associated with sensor movements reveals a highly cooperative transition over a limited voltage range (Ledwell and Aldrich 1999; Loboda and Armstrong 2001; Schoppa and Sigworth 1998).

The last two helices and the included loop contribute to the lining of the aqueous pore. The structure of a bacterial channel, KcsA, which consists of just these three elements, has been solved (Doyle et al. 1998; Zhou et al. 2001) and is being mined for insights into the manner in which ions traverse the membrane (Perozo et al. 1999)

and the process of selectivity (Morais-Cabral et al. 2001). The last helix, S6, is arranged in a teepee-like structure where the "smoke hole" constitutes the narrowest point of the channel pore, called the activation gate (Yellen 1998). Movements of S5 and S6 helices have been shown to underlie the closed to open transition (Fedida and Hesketh 2001; Holmgren et al. 1998; Liu et al. 1997; Shieh et al. 1997). In addition, residues on the S5 helix have also been shown to stabilize the channel open state (Kanevsky and Aldrich 1999). An analysis of gating currents reveals that channel gating is also a highly co-operative phenomenon in most K^+ channels. However, the detailed mechanics of the manner in which movement of the voltage sensor S4 is transduced into S5/S6 movement and hence channel opening is unknown.

Both N- and C-termini of these membrane proteins are cytoplasmic and a growing body of evidence suggests that they interact with each other (Schulteis et al. 1996) and with the transmembrane region to modulate Kv channel assembly, gating and permeation (Hopkins et al. 1994). The resulting alterations in physiology have been shown to be responsible for a range of channelopathies. Deletions in the N-terminus remove inactivation (Hoshi et al. 1990) and have also been shown to affect both the rate and voltage dependence of activation (Hollerer-Beitz et al. 1999; Pascual et al. 1997; VanDongen et al. 1990). Similarly, in the case of six transmembrane inward-rectifiers like KAT1 and HERG, the N-terminus influences the gating properties and its deletion gives rise to altered voltage dependence of activation (Marten and Hoshi 1997, 1998; Viloria et al. 2000) and of deactivation (Wang et al. 2000). These amino terminal effects on activation gating can be suppressed by second-site mutations in S4, the voltage sensor (Terlau et al. 1997). Point mutations in the N-terminal T0 domain perturb the ionic conductance and pharmacology of Kv1.3 (Yao et al. 2000). Besides, the distal N-terminal domains of Kv1.4 have been shown to interact directly with alpha-actin and have been implicated in membrane anchoring of the channel and current density (Cukovic et al. 2001).

We have earlier reported on chimæric channel constructs where aberrant interactions between transplanted N-terminal cytoplasmic residues and the transmembrane body result in either altered cooperativity of the gating transition (Varshney and Mathew 2000) or in a shift in the operating range of the channel (Chanda et al. 1999a, 1999b). In an extension of these demonstrations of the ability of N-terminal residues to modulate channel gating, we now present data on another chimæric channel in which these interactions perturb the mechanism(s) by which the channel is locked into the open state on depolarization.

Materials and methods

Isolation and maintenance of *Xenopus* oocytes

Oocytes were isolated by mini-laparotomy from adult female *Xenopus laevis*. The frogs were anaesthetized by immersion in 0.04% benzocaine for 15–20 min, then placed on a wet platform during dissection and removal of ovarian lobes. The incision was sutured closed and the frog was allowed to recover for about two months before removal of another batch of oocytes. Clusters of oocytes were treated with 1 mg/mL type 1A collagenase (Sigma) in OR-Mg solution that contained (mM): 82 NaCl, 2 KCl, 20 $MgCl_2$, 5 HEPES (pH 7.7). The isolated oocytes were then incubated for microinjection at 18 °C in ND96-HS solution containing (mM): 96 NaCl, 2 KCl, 1.8 $CaCl_2$, 1 $MgCl_2$, 5 HEPES, 2.5 Na-pyruvate (pH 7.7) supplemented with 100 U/mL of Pen-Strep and 5% heat-inactivated horse serum.

Molecular biology

The potassium channel cDNAs were subcloned into pGEMA (Ramaswami et al. 1990). Both hKv1.1 and hKv1.2 have unique *Sca*I sites at respectively 86 and 87 amino residues upstream of the first transmembrane segment, S1. The N-terminal fragment from hKv1.1 was excised and transplanted onto hKv1.2 at the *Sca*I site, as shown in Fig. 1. The resulting construct, 1N/2, contains 80 amino acid residues of the N-terminus of hKv1.1 linked to 425 residues of hKv1.2.

Δ75N2 was generated by using PCR techniques; the upper mutagenic primer, 5′-CCCTCTCTAGAATGTTTTTCGATC-3′, binds at position 212 bp, contains an *Xba*I site and generates methionine as the 75th residue; the lower primer, 5′-TAT-CTTTCCCCCCAATGGT-3′, binds at the 3′-position 1150 bp in the hKv1.2 template. The PCR was carried out using Pfu DNA polymerase (Promega) at an annealing temperature of 52 °C. The 948 bp PCR product was digested with *Xba*I and *Bst*EII restriction endonucleases, generating a 320 bp DNA fragment that was subsequently gel eluted and ligated to the *Xba*I-*Bst*EII backbone of hKv1.2. The resultant construct, Δ75N2, has a deletion of 75 N-terminal residues of hKv1.2, leaving 87 cytoplasmic residues before S1. The mutagenesis was confirmed by sequencing on an ABI PRISM 310 automated sequencer.

Capped polyadenylated RNA of hKv1.1, hKv1.2, 1N/2 and Δ75N2 was generated using T7 RNA polymerase (mMessage

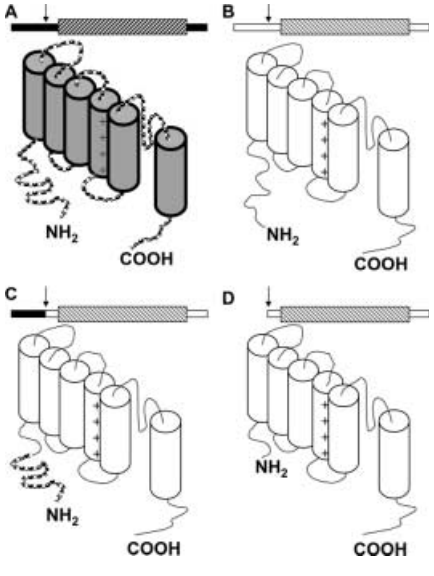

Fig. 1A–D. Schematic representation of K^+ channel topologies. Transmembrane topologies and bar diagrams of (**A**) hKv1.1, (**B**) hKv1.2, (**C**) a chimæra 1N/2 generated by transplanting 80 residues (shown as *beaded line*) from the N-terminus of hKv1.1 onto the transmembrane portion of hKv1.2, and (**D**) a deletion construct Δ75N2 of hKv1.2 starting at the point of fusion, which is shown by an *arrow* in the bar diagrams. The *shaded area* in the bar diagrams depicts the transmembrane region of the channel protein

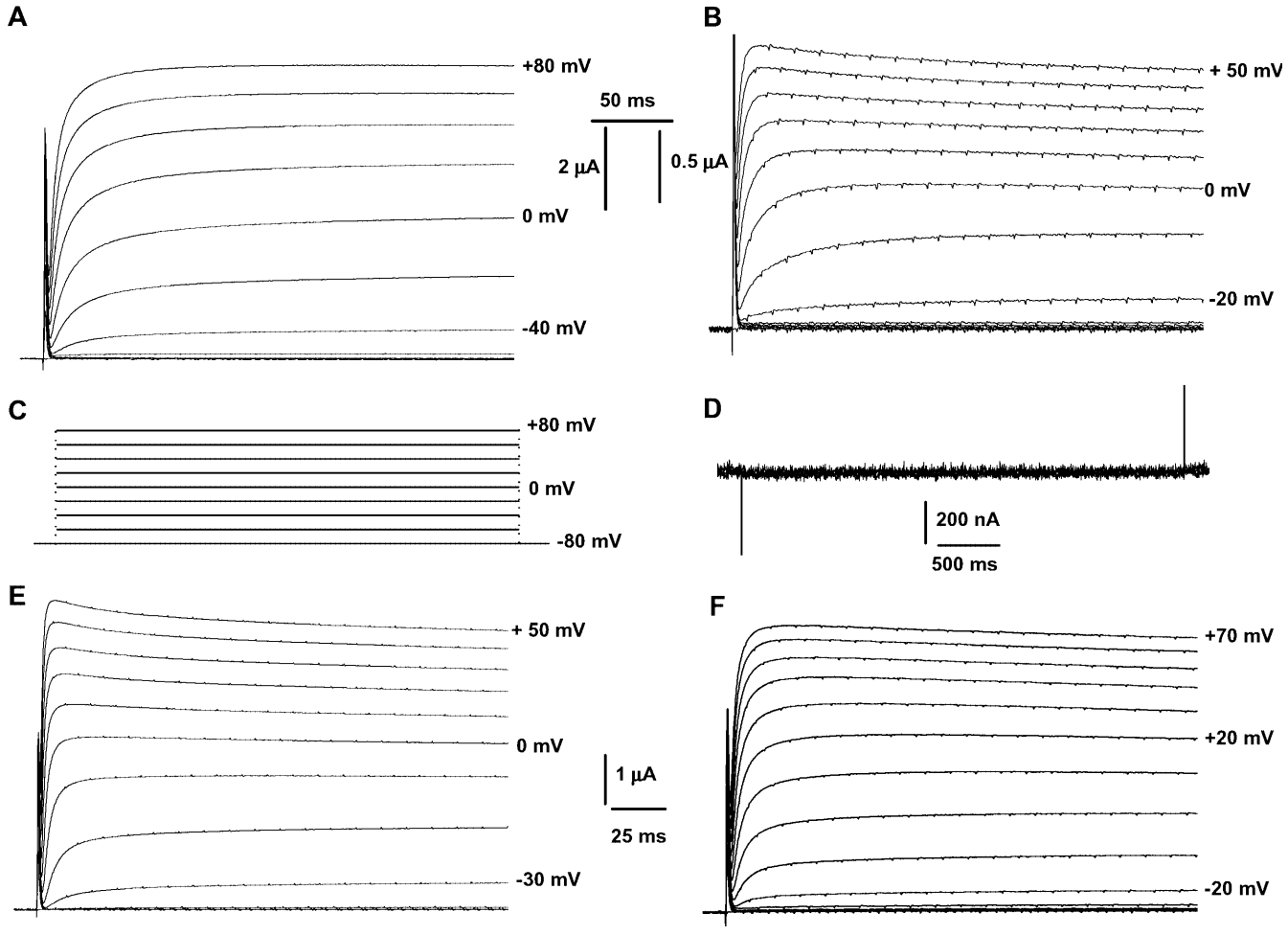

Fig. 2A–F. Currents from oocytes expressing K^+ channel constructs. Currents elicited in oocytes expressing (**A**) hKv1.1, (**B**) hKv1.2, (**E**) the 1N/2 chimæra and (**F**) Δ75N2 on depolarizing from –80 mV. Oocytes expressing these channels were held at –80 mV following a pulse protocol shown in **C** and subjected to a 1 s hyperpolarizing pre-pulse of –120 mV (not shown) prior to depolarizing to potentials indicated against the traces. **D** Inward currents through 1N/2 chimæra or Δ75N2 in response to hyperpolarizing pulses. Oocytes were held at –60 mV and stepped to hyperpolarizing potentials from –60 to –140 mV in –10 mV steps

mMachine transcription kit, Ambion, USA). 46 nL of transcribed RNA (150–300 ng/µL) was injected per oocyte. Electrophysiological recordings were carried out 2–5 days after injection.

Electrophysiology

Methods for RNA injection and the two-electrode voltage clamp of *Xenopus* oocytes have been described (Ramaswami et al. 1990). In short, we used an OC-725 oocyte clamp amplifier (Warner Instruments) to maintain the holding potentials and record membrane currents. The external recording solution was modified ND96, containing (mM): 96 sodium gluconate, 2 potassium gluconate, 1.8 calcium gluconate, 1 magnesium gluconate, 5 HEPES (pH 7.7). Solution exchange was achieved by gravity flow. Analogue data from the amplifier were sampled at 5–15 kHz and filtered at 2–5 kHz by a low-pass filter (LPF-100, Warner Instruments), digitized and stored on a 486 PC hard disk for further analysis. The PCLAMP 6.0 (Axon Instruments) software package was used to generate voltage-clamp commands, acquire membrane currents and analyse digitized data. Charybdotoxin (CTX) was acquired from Sigma and 100 µM stock made in 0.1 mg/mL BSA solution with 10 mM HEPES buffer (pH 7.6). All experiments were performed at room temperature.

Data analysis and numerical calculations

All experimental data were first analysed with Clampfit 6.0 and exported to SigmaPlot 5.0 or Origin 6.0 for subsequent analysis, curve fitting and display. Voltage-dependent activation curves are best fits to the Boltzmann function $[G = G_{max}/\{1 + \exp(V_{1/2} - V)/a\}]$, where G is the conductance at potential V, G_{max} the maximum conductance observed, $V_{1/2}$ the mid point of activation, and a the slope factor. Voltage-dependent rising and decaying phases of potassium currents were fitted to single or double exponential functions to obtain rates of activation and deactivation. The concentration dependence of the CTX block was fitted to a form of the Langmuir equation, $I/I_0 = I_0/\{1 + ([CTX]/IC_{50})\}$, where I_0 is the current in the absence of CTX, I the observed current in the presence of [CTX] at different concentrations (nM), and IC_{50} the concentration of CTX required for 50% block.

Results

Perturbation techniques have proven very useful in assigning functional roles to different portions of the channel protein. Molecular biological manipulation

followed by expression in heterologous systems and subsequent electrophysiological characterization has been the approach of choice. One of the most frequently used expression systems is the *Xenopus* oocyte, which does not exhibit significant time- or voltage-dependent K^+-selective currents on its own (Dascal et al. 1986). We have previously shown that oocytes expressing hKv1.1 or hKv1.2 exhibit non-inactivating outward currents on depolarization, while hKv1.4-expressing oocytes exhibit rapidly inactivating outward currents (Ramaswami et al. 1990). Figure 1 presents schematic representations of the transmembrane topologies of hKv1.1, hKv1.2, the chimæric construct 1N/2 and the truncation product Δ75N2, which has been truncated at the junction of the chimæra.

Figure 2 presents currents elicited by depolarizing pulses delivered to oocytes expressing the various constructs under study: hKv1.1 (Fig. 2A), hKv1.2 (Fig. 2B), the 1N/2 chimæra (Fig. 2E) and the truncation product Δ75N2, which is hKv1.2 truncated at the junction of the chimæra (Fig. 2F). Swapping the N-terminal tail of hKv1.4 onto the body of hKv1.1 has been shown to generate an inward rectifier (Chanda et al. 1999a, 1999b). Hence, we have looked for inward currents on hyperpolarizing oocytes expressing the chimæra. Non-inactivating, outward currents are observed as expected for the chimæra and for the truncation product. No inward currents were, however, observed on hyperpolarizing these oocytes (Fig. 2D). The currents observed in oocytes expressing the chimæra are K^+-selective, as seen from the reversal potential of ca. –90 mV (Fig. 3B), which is indistinguishable from that determined for both parental channels in a bathing medium of 2 mM K^+ (Ramaswami et al. 1990). Moreover, the currents can be blocked by CTX, a peptide blocker for Kv1.2 channels (Guillemare et al. 1992; Ramaswami et al. 1990) (Fig. 3A). Since CTX blocks Kv1.2 channels at sub-micromolar concentrations but does not affect hKv1.1 channels at these concentrations, this result establishes that the ion-conducting pore in the 1N/2 chimera is derived from hKv1.2.

On plotting the normalized conductance (G/G_{max}) of 1N/2 currents against transmembrane potential (V) (Fig. 4A), it is clear that the voltage dependence of channel opening is shifted by 25 mV to hyperpolarizing potentials in the case of the chimæra compared to hKv1.2. This shift is not caused by the loss of the N-terminal cytoplasmic tail of hKv1.2 as the truncation product, Δ75N2, does not exhibit such a shift. On the other hand, both the truncation product and the chimæra exhibit distinct maxima (at +30 mV and at 0 mV, respectively) in their G-V curves in contrast to hKv1.1 or hKv1.2 (Fig. 4A). The decline in conductance seen on depolarizing the chimæra beyond +5 mV is not a voltage clamp artefact, as no such decline is seen in oocytes expressing hKv1.1 or hKv1.2 at similar current levels. This decline in conductance implies that the chimæric channels enter a non-conducting or a sub-conductance state on depolarizing above +10 mV. If this decline in conductance is due to some channels going into an inactivated state, recovery from this state would be expected to be favoured at hyperpolarizing potentials. Following hyperpolarizing pre-pulses of 500 ms ranging from –110 mV to –140 mV, current traces at the test

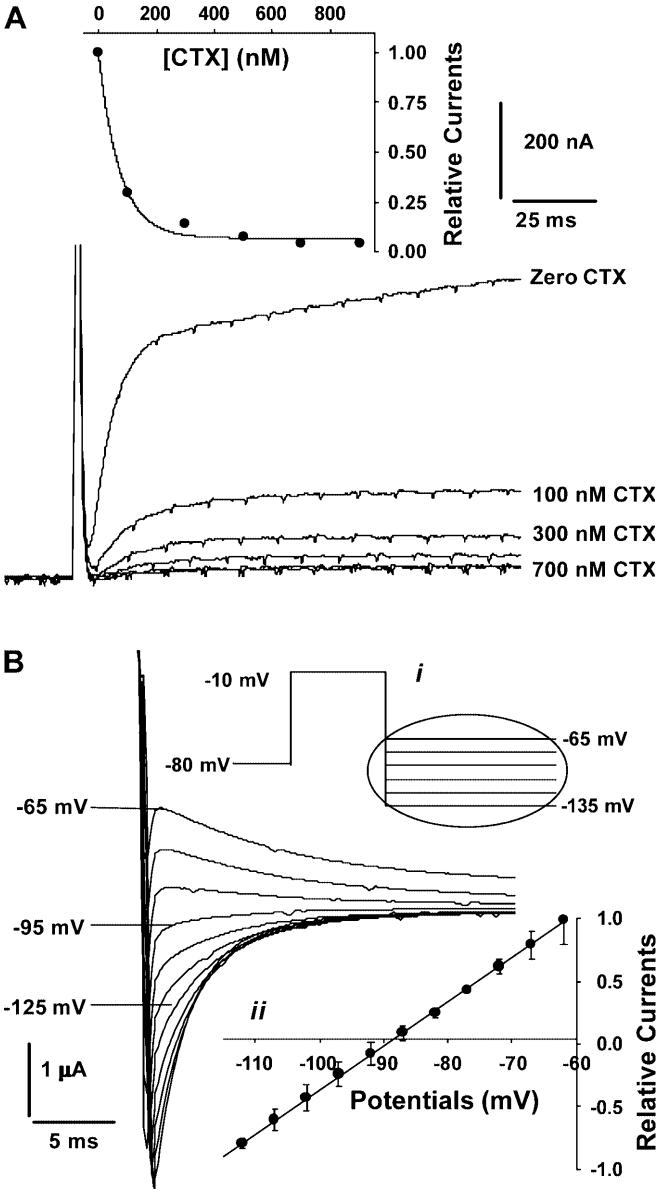

Fig. 3A, B. Pharmacology and selectivity of K^+ currents. **A** The concentration dependence of a charybdotoxin (CTX) block of the K^+ current of the 1N/2 chimæra. CTX was applied in a cumulative fashion to an oocyte expressing the 1N/2 chimæra; the test potential was –10 mV and currents were recorded at different concentrations after the manual addition of CTX to the bath. *Inset* plots currents as a function of CTX concentration, yielding an IC_{50} of 72 nM. **B** Reversal potential for 1N/2 chimæra in 2 mM $[K^+]_{out}$. Channels were opened at –10 mV for 200 ms, and then stepped to different repolarizing potentials ranging from –135 mV to –65 mV for 100 ms, as shown in *inset i*. Tail current amplitude through closing channels was determined by fitting the current between 5 and 100 ms after repolarization to a single exponential function and then extrapolating back to the start of the repolarization step. *Inset ii* shows the variation of this tail current amplitude with repolarizing potentials

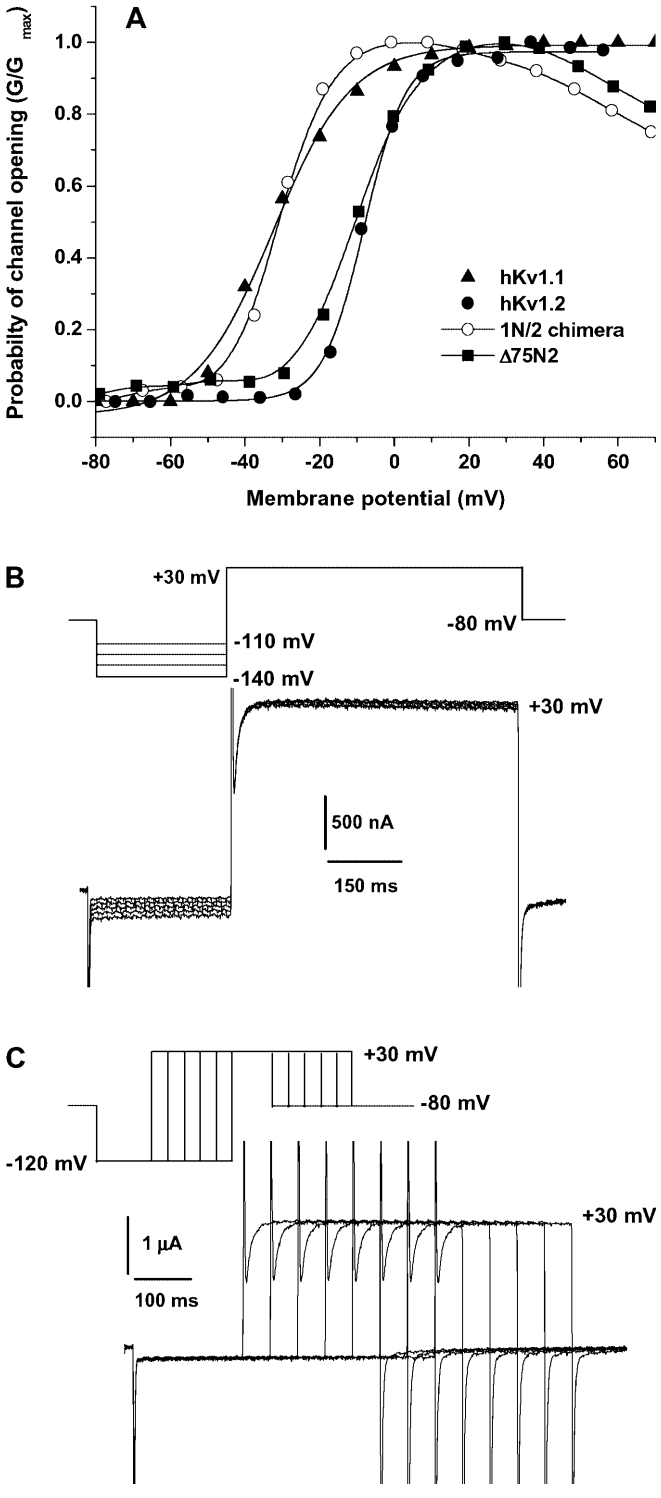

◀

Fig. 4A–C. Voltage dependence of K^+ currents. **A** Voltage-dependent activation of the 1N/2 chimæra (*open circles*), hKv1.1 (*triangles*), hKv1.2 (*filled circles*) and Δ75N2 (*squares*). The curves through the data points are the best fits to Boltzmann functions. $V_{1/2}$ of activation for 1N/2 chimæra, hKv1.1, hKv1.2 and Δ75N2 are –32, –31, –7 and –9 mV, respectively. Data points represent means of several independent acquisitions ($n \geq 4$ for all data sets). Pre-pulse conditioning of 1N/2 currents by varying pre-pulse potential (**B**) and pre-pulse time (**C**). **B** Oocytes expressing the 1N/2 chimæra were held at a range of potentials from –110 mV to –140 mV for 400 ms before stepping to the common test potential of +30 mV, as shown in the inset. In the other experiment, (**C**) the oocyte was held at –120 mV for varied time periods from 200 ms to 600 ms before stepping to the common test potential of +30 mV, as shown in the inset

potential of +30 mV were superimposable (Fig. 4B), indicating that recovery, if any, was complete at all pre-pulse potentials. Similarly, the duration of the pre-pulse potential at –120 mV was varied from 200 ms to 600 ms and again all the traces at the test potential of +30 mV were superimposable (Fig. 4C), indicating that all the channels were in the closed state after even the briefest of the pre-pulses used.

The state that the chimæra enters at potentials above +5 mV could be either an inactive state or a closed state (deactivated). We have used a three-step pulse protocol to distinguish between these possibilities. Channels are equilibrated at a holding potential (V1), stepped to a series of potentials ranging from –45 mV to +40 mV (V2) and then taken back to a test potential which is identical to the initial holding potential (V3, which is the same potential as for V1) (Fig. 5A). If the channels were inactivating during the intermediate pulse V2, then on being brought back to the test potential in V3 there would be fewer channels capable of opening, and hence the current amplitude would be lower than that in the initial holding step V1. The pulse protocol was run for a series of test potentials ranging from –35 mV to +15 mV.

The data in Fig. 5B show the current traces obtained with an oocyte held at –25 mV (V1) and taken through a series of intervening pulses (V2) from –45 mV to +40 mV before stepping back to –25 mV (V3). In all cases, the current before and after the intervening pulse was the same, indicating that no inactivation had occurred. Since the intervening pulse took the oocytes to potentials on either side of the potential for maximum conductance, it would appear that the decline in conductance above the maximum cannot be ascribed to inactivation. For intervening pulses V2 between +40 mV and –20 mV, a return to the test potential, V3, of –25 mV involves in a decrease in current. The time constants of this decay are presented in Fig. 5B (inset *i*), and found to be independent of the pre-pulse potential. Conversely, for intervening pulses between –30 mV and –45 mV, a return to the test potential of –25 mV involves an increase in current. Here, the rate of current rise did depend on the pre-pulse potential, increasing with increasing depolarization during V2 (Fig. 5B, inset *ii*).

The rate of current rise on stepping to a test pulse of +15 mV from a range of holding potentials (V_{HOLD}) could depend on the history of the sample prior to attaining the holding potential. We contrast the behaviour of channels brought to the holding potential from the closed state at –80 mV to those brought to the holding potentials from +15 mV, a potential beyond the conductance maximum (Fig. 5C). The manner in which the samples were brought to the holding potential made no

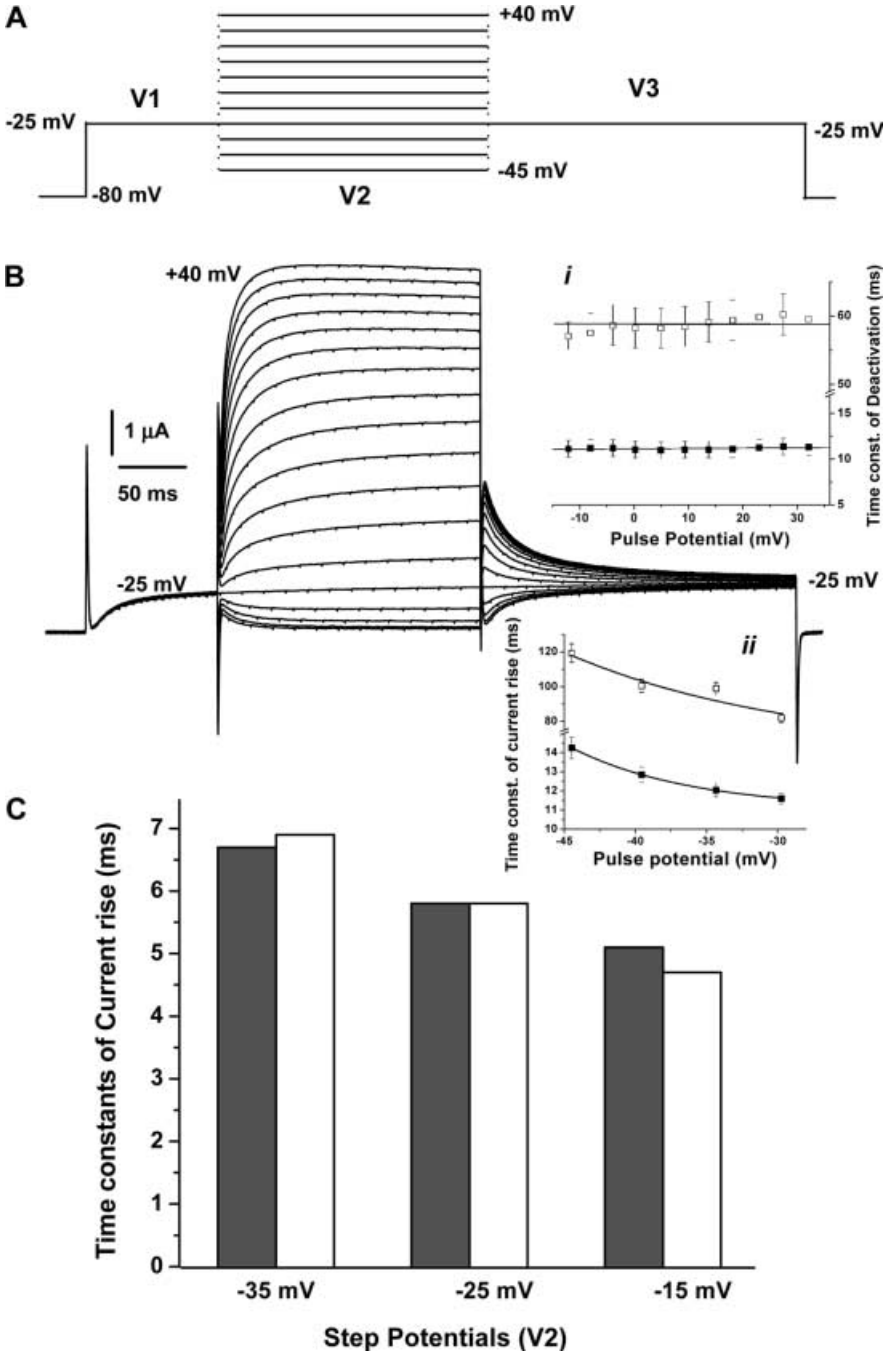

Fig. 5A–C. Inactivation or deactivation? Oocytes expressing the 1N/2 chimæra were subjected to a three-step pulse protocol (**A**). Oocytes were held at –80 mV and stepped to a holding potential (V1) ranging from –35 mV to +15 mV. After 100 ms at this potential, they were stepped to a range of potentials (V2) from –45 mV to +40 mV for 200 ms. They were then taken to the test potential (V3), which is the same as the holding potential in the first pulse, for 250 ms. **B** Currents recorded from an oocyte subjected to the pulse protocol with a test potential of –25 mV. The currents during the first 100 ms of the third pulse V3 were fitted to double exponential decays. The time constants of this decay are presented as a function of the pre-pulse potential V2 in *inset i*. Current rise for the last four traces were similarly fitted and *inset ii* presents both of the time constants of the fit ($n=3$). **C** Time constants for current rise to a test potential of +15 mV from –35, –25 and –15 mV holding potentials (V_{HOLD}). *Black bars* are for channels brought to V_{HOLD} from –80 mV (–80 mV → V_{HOLD} → +15 mV); *white bars* from +15 mV (+15 mV → V_{HOLD} → +15 mV)

significant difference to the rate of current rise to +15 mV in any of the instances tested.

Discussion

The mapping of specific functions onto distinct regions of the K^+ channel has been carried out in large part using the *Drosophila* channel Shaker as the model. Variation in Shaker is brought about by alternative splicing, with all transcripts sharing the central region consisting of the transmembrane portion and a stretch of the N-terminus, which includes the T1 domain (Iverson et al. 1988; Kamb et al. 1988). Mammalian channels, on the other hand, are encoded on separate genes without such strict conservation of the transmembrane region (Stuhmer et al. 1989). Thus domain swaps in mammalian channels can bring about novel interactions within the chimæras created (Stocker et al. 1991). We have previously reported on two such aberrant interactions: the 1N/4 chimæra where cooperativity in channel opening is affected (Varshney and Mathew 2000) and the 4N/1 chimæra where the operating range of the channel is altered (Chanda et al. 1999a, 1999b). The 1N/2 chimæra we report on here is another instance of an aberrant interaction demonstrating that N-terminal

cytoplasmic residues can influence the voltage dependence of channel opening.

The normalized conductance-voltage curve for the 1N/2 chimæra displays a distinct maximum at 0 mV, unlike other Kv channels which achieve a plateau conductance on depolarization. The decrease in conductance is due to channels entering either a non-conducting state or a sub-conductance state on further depolarization. The two-electrode voltage clamp technique cannot distinguish between these alternatives. However, the kinetics of reopening can distinguish between inactive states versus closed states or sub-conductance states from which a transition to the "fully open" state is facile. The pulse protocol in Fig. 5 makes an estimate of the number of channels capable of opening from a holding potential of –80 mV, a fixed proportion of which open on depolarizing to the initial pulse potential V1 (–25 mV in Fig. 5B). If some of these channels inactivate on holding at the higher potentials in the intermediate pulse V2, a smaller current would be expected on stepping to the test potential V3. However, no such decline is observed at any of the test potentials.

The rate of channel closing should be dependent only on the potential at which the channels deactivate, if they all close from the same open state. Indeed, the rate of current decay from each of the intermediate potentials V2 to the holding potential (–25 mV in this case) is the same (inset *i* to Fig. 5B). The kinetics of channel opening has been modelled with a series of closed states existing in voltage-dependent equilibrium leading to a single open state (Zheng and Sigworth 1998). Holding at depolarized potentials should populate closed states close to the final opening transition. Opening from these states should be more rapid than opening from states farther from the transition. The observed kinetics of opening is consistent with this scheme (inset *ii* to Fig. 5B) and reflects the population of states present prior to the depolarizing pulse.

We have delivered depolarizing pulses to channels held at a series of potentials (V_{HOLD}) and monitored the kinetics of current rise at +15 mV (Fig. 5). Channels were brought to the pre-pulse potentials either from –80 mV, where all the channels were in closed states, or from +15 mV, where ~10% of the channels are in a non-conducting state. In the former case the transition followed was from V1 to V2, while in the latter it was from V2 to V3. However, the kinetics of current rise are the same in both cases (Fig. 5C). This, in turn, requires that transitions from the non-conducting state at +15 mV to open and closed states be facile. Hence, it is unlikely that the decline in conductance at +15 mV is due to 10% of the channels entering an inactive state.

The *G-V* curves of hKv1.2 and 1N/2 differ in two respects: the shift in voltage dependence is due to the interaction of the foreign hKv1.1-derived chain with the body of hKv1.2, as no shift is seen in the deletion construct Δ75N2. On the other hand, the decline in conductance on extensive depolarization is seen both the in Δ75N2 and in the 1N/2 chimæra, suggesting that the native N-terminal chain of hKv1.2 is responsible for locking the channel into its normal open state.

Channel opening is accompanied by changes in the inter-helix distances of the S6 helix, interpreted as a rotation of S6 leading to a widening of the "smoke hole" in the teepee structure (Liu et al. 1997; Yellen 1998). It is conceivable that the decline in conductance we see is due to over-rotation of this helix. A simple model building exercise reveals that rotation of S6s from the closed state results in increasing the diameter of the smoke hole to a maximum, followed by a decreasing diameter on further rotation. Knobs into holes packing of helices would normally permit only a limited range of helix crossing angles and such extensive rearrangement may be energetically unfavourable. However, studies of distances between points on S6 suggest considerable scope for movement (del Camino and Yellen 2001). If so, limits are probably imposed on the movement of S4 or S6 or both. The breakdown of these limiting mechanisms in the 1N/2 chimæra could provide a handle to identify the elements of the machinery that transduces movements of the voltage sensor into channel opening.

Acknowledgements A.V. acknowledges support from the Kanwal Rekhi Scholarship of the TIFR Endowment Fund. This work was supported by internal funds from NCBS-TIFR.

References

Antz C, Geyer M, Fakler B, Schott MK, Guy HR, Frank R, Ruppersberg JP, Kalbitzer HR (1997) NMR structure of inactivation gates from mammalian voltage-dependent potassium channels. Nature 385:272–275

Bezanilla F (2000) The voltage sensor in voltage-dependent ion channels. Physiol Rev 80:555–592

Cha A, Snyder GE, Selvin PR, Bezanilla F (1999) Atomic scale movement of the voltage-sensing region in a potassium channel measured via spectroscopy. Nature 402:809–813

Chanda B, Tiwari JK, Varshney A, Mathew MK (1999a) Exploring the architecture of potassium channels using chimeras to reveal signal transduction. Biosci Rep 9:301–306

Chanda B, Tiwari JK, Varshney A, Mathew MK (1999b) Transplanting the N-terminus from Kv1.4 to Kv1.1 generates an inwardly rectifying K^+ channel. Neuroreport 10:237–241

Cukovic D, Lu GW, Wible B, Steele DF, Fedida D (2001) A discrete amino terminal domain of Kv1.5 and Kv1.4 potassium channels interacts with the spectrin repeats of alpha-actinin-2. FEBS Lett 498:87–92

Dascal N, Snutch TP, Lubbert H, Davidson N, Lester HA (1986) Expression and modulation of voltage-gated calcium channels after RNA injection in *Xenopus* oocytes. Science 231:1147–1150

del Camino D, Yellen G (2001) Tight steric closure at the intracellular activation gate of a voltage-gated K^+ channel. Neuron 32:649–656

Doyle DA, Cabral JM, Pfuetzner RA, Kuo A, Gulbis JM, Cohen SL, Chait BT, MacKinnon R (1998) The structure of the potassium channel: molecular basis of K^+ conduction and selectivity. Science 280:69–77

Fedida D, Hesketh JC (2001) Gating of voltage-dependent potassium channels. Prog Biophys Mol Biol 75:165–199

Guillemare E, Honore E, Pradier L, Lesage F, Schweitz H, Attali B, Barhanin J, Lazdunski M (1992) Effects of the level of mRNA expression on biophysical properties, sensitivity to neurotoxins,

and regulation of the brain delayed-rectifier K^+ channels Kv1.2. Biochemistry 31:12463–12468
Hollerer-Beitz G, Schonherr R, Koenen M, Heinemann SH (1999) N-Terminal deletions of rKv1.4 channels affect the voltage dependence of channel availability. Pflugers Arch 438:141–146
Holmgren M, Shin KS, Yellen G (1998) The activation gate of a voltage-gated K^+ channel can be trapped in the open state by an intersubunit metal bridge. Neuron 21:617–621
Hopkins WF, Demas V, Tempel BL (1994) Both N- and C-terminal regions contribute to the assembly and functional expression of homo- and heteromultimeric voltage-gated K^+ channels. J Neurosci 14:1385–1393
Hoshi T, Zagotta WN, Aldrich RW (1990) Biophysical and molecular mechanisms of Shaker potassium channel inactivation. Science 250:533–538
Iverson LE, Tanouye MA, Lester HA, Davidson N, Rudy B (1988) A-type potassium channels expressed from Shaker locus cDNA. Proc Natl Acad Sci USA 85:5723–5727
Kamb A, Tseng-Crank J, Tanouye MA (1988) Multiple products of the *Drosophila* Shaker gene may contribute to potassium channel diversity. Neuron 1:421–430
Kanevsky M, Aldrich RW (1999) Determinants of voltage-dependent gating and open-state stability in the S5 segment of Shaker potassium channels. J Gen Physiol 114:215–242
Ledwell JL, Aldrich RW (1999) Mutations in the S4 region isolate the final voltage-dependent cooperative step in potassium channel activation. J Gen Physiol 113:389–414
Liu Y, Holmgren M, Jurman ME, Yellen G (1997) Gated access to the pore of a voltage-dependent K^+ channel. Neuron 19:175–184
Loboda A, Armstrong CM (2001) Resolving the gating charge movement associated with late transitions in K^+ channel activation. Biophys J 81:905–916
Mannuzzu LM, Moronne MM, Isacoff EY (1996) Direct physical measure of conformational rearrangement underlying potassium channel gating. Science 271:213–216
Marten I, Hoshi T (1997) Voltage-dependent gating characteristics of the K^+ channel KAT1 depend on the N and C termini. Proc Natl Acad Sci USA 94:3448–3453
Marten I, Hoshi T (1998) The N-terminus of the K channel KAT1 controls its voltage-dependent gating by altering the membrane electric field. Biophys J 74:2953–2962
Morais-Cabral JH, Zhou Y, MacKinnon R (2001) Energetic optimization of ion conduction rate by the K^+ selectivity filter. Nature 414:37–42
Pascual JM, Shieh CC, Kirsch GE, Brown AM (1997) Contribution of the NH_2 terminus of Kv2.1 to channel activation. Am J Physiol 273:C1849–C1858
Perozo E, Cortes DM, Cuello LG (1999) Structural rearrangements underlying K^+ channel activation gating. Science 285:73–78
Ramaswami M, Gautam M, Kamb A, Rudy B, Tanouye MA, Mathew MK (1990) Human potassium channel genes: molecular cloning and functional expression. Mol Cell Neurosci 1:214–223
Schoppa NE, Sigworth FJ (1998) Activation of Shaker potassium channels. III. An activation gating model for wild-type and V2 mutant channels. J Gen Physiol 111:313–342
Schulteis CT, Nagaya N, Papazian DM (1996) Intersubunit interaction between amino- and carboxyl-terminal cysteine residues in tetrameric Shaker K^+ channels. Biochemistry 35:12133–12140
Shieh CC, Klemic KG, Kirsch GE (1997) Role of transmembrane segment S5 on gating of voltage-dependent K^+ channels. J Gen Physiol 109:767–778
Stocker M, Pongs O, Hoth M, Heinemann SH, Stuhmer W, Schroter KH, Ruppersberg JP (1991) Swapping of functional domains in voltage-gated K^+ channels. Proc R Soc Lond Ser B 245:101–107
Stuhmer W, Ruppersberg JP, Schroter KH, Sakmann B, Stocker M, Giese KP, Perschke A, Baumann A, Pongs O (1989) Molecular basis of functional diversity of voltage-gated potassium channels in mammalian brain. EMBO J 8:3235–3244
Terlau H, Heinemann SH, Stuhmer W, Pongs O, Ludwig J (1997) Amino terminal-dependent gating of the potassium channel rat eag is compensated by a mutation in the S4 segment. J Physiol (Lond) 502:537–543
VanDongen AM, Frech GC, Drewe JA, Joho RH, Brown AM (1990) Alteration and restoration of K^+ channel function by deletions at the N- and C-termini. Neuron 5:433–443
Varshney A, Mathew MK (2000) Cytoplasmic residues influence the voltage-dependence of the gating of human K^+ channels. Neuroreport 11:2913–2917
Viloria CG, Barros F, Giraldez T, Gomez-Varela D, de la Pena P (2000) Differential effects of amino-terminal distal and proximal domains in the regulation of human erg K^+ channel gating. Biophys J 79:231–246
Wang J, Myers CD, Robertson GA (2000) Dynamic control of deactivation gating by a soluble amino-terminal domain in HERG K^+ channels. J Gen Physiol 115:749–758
Yao X, Liu W, Tian S, Rafi H, Segal AS, Desir GV (2000) Close association of the N terminus of Kv1.3 with the pore region. J Biol Chem 275:10859–10863
Yellen G (1998) The moving parts of voltage-gated ion channels. Q Rev Biophys 31:239–295
Zagotta WN, Hoshi T, Aldrich RW (1990) Restoration of inactivation in mutants of Shaker potassium channels by a peptide derived from ShB. Science 250:568–571
Zheng J, Sigworth FJ (1998) Intermediate conductances during deactivation of heteromultimeric Shaker potassium channels. J Gen Physiol 112:457–474
Zhou Y, Morais-Cabral JH, Kaufman A, MacKinnon R (2001) Chemistry of ion coordination and hydration revealed by a K^+ channel-Fab complex at 2.0 Å resolution. Nature 414:43–48